New Journal of Physics
The open access journal at the forefront of physics

Deutsche Physikalische Gesellschaft DPG
IOP Institute of Physics

Published in partnership with: Deutsche Physikalische Gesellschaft and the Institute of Physics

PAPER

An efficient nonlinear Feshbach engine

Jing Li[1], Thomás Fogarty[2], Steve Campbell[3], Xi Chen[1] and Thomas Busch[2,4]

[1] Department of Physics, Shanghai University, 200444, Shanghai, People's Republic of China
[2] Quantum Systems Unit, Okinawa Institute of Science and Technology Graduate University, Okinawa, 904-0495, Japan
[3] Instituto Nazionale di Fisica Nucleare, Sezione di Milano, & Dipartimento di Fisica, Università degli Studi di Milano, Via Celoria 16, I-20133 Milan, Italy
[4] Author to whom any correspondence should be addressed.

E-mail: xchen@shu.edu.cn **and** thomas.busch@oist.jp

Keywords: shortcut to adiabaticity, quantum thermodynamics, Otto cycle, soliton matter wave

OPEN ACCESS

RECEIVED
7 September 2017

REVISED
6 November 2017

ACCEPTED FOR PUBLICATION
23 November 2017

PUBLISHED
9 January 2018

Abstract

We investigate a thermodynamic cycle using a Bose–Einstein condensate (BEC) with nonlinear interactions as the working medium. Exploiting Feshbach resonances to change the interaction strength of the BEC allows us to produce work by expanding and compressing the gas. To ensure a large power output from this engine these strokes must be performed on a short timescale, however such non-adiabatic strokes can create irreversible work which degrades the engine's efficiency. To combat this, we design a shortcut to adiabaticity which can achieve an adiabatic-like evolution within a finite time, therefore significantly reducing the out-of-equilibrium excitations in the BEC. We investigate the effect of the shortcut to adiabaticity on the efficiency and power output of the engine and show that the tunable nonlinearity strength, modulated by Feshbach resonances, serves as a useful tool to enhance the system's performance.

1. Introduction

The ability to accurately control quantum systems using the latest available experimental techniques has opened the door to thinking about experiments which can study the nature of thermodynamics in the quantum realm [1–4]. In particular, it is interesting to study conceptual heat engines, which are systems governed by a complex dynamics and in which the manipulation of quantum states can be used to produce work. Due to the recent progress in precisely controlling the non-adiabatic dynamics of ultracold atoms and Bose–Einstein condensates (BECs) [5–9], and the ability to tune many of their system parameters, they offer ideal systems with which to create quantum heat engines [10–12].

To do work in a heat cycle, the Hamiltonian must be modified as adiabatically as possible to avoid unwanted excitations. This, however, requires long timescales which can have drawbacks, such as exceeding the life time of cold atom systems and having a low output power. One method to circumvent this issue is to use a shortcut to adiabaticity (STA) [13, 14], which allows for fast quantum state manipulation while also suppressing final excitations [15–17]. Techniques such as quantum transitionless driving (or counter-diabatic driving), fast-foward algorithms, and inverse engineering have been shown to yield states with high fidelity in finite time, see the recent reviews [18, 19]. While these approaches have often centered around non-interacting systems, STAs have also been explored in interacting, nonlinear, and other systems [20–25]. Remarkably, STAs have fundamental implications on quantum speed limits (QSL) [26–30], time-energy uncertainty relations (or energy cost) [31–38], and the quantification of the third law of thermodynamics in the context of quantum refrigerators [39, 40], which results in intriguing practical applications in heat engines [41–47].

In this work we analyze a quantum Otto cycle [48–55], (see figure 1) that uses a BEC with attractive nonlinear interactions, which can be described as a bright soliton, as its working medium. The creation and control of bright solitons in BECs is well established experimentally [56–61], making it an ideal nonlinear interacting system to investigate. Rather than using the STA to modulate the trapping potential and therefore do work on the system, as has been investigated previously for example in [41–45], we instead fix the trapping frequency and

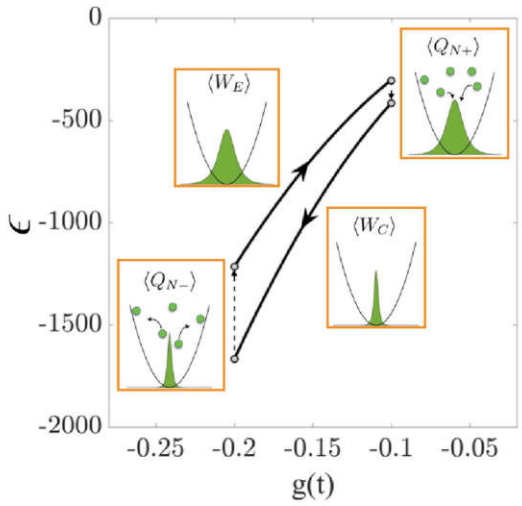

Figure 1. Otto cycle: work is done during the compression $\langle W_C \rangle$ and expansion strokes $\langle W_E \rangle$. Through coupling to an external reservoir the number of particles, N, can be increased or decreased, thereby dissipating particles $\langle Q_{N-} \rangle$ and absorbing particles $\langle Q_{N+} \rangle$ and therefore increasing or decreasing the energy.

compress and expand the soliton by time dependently varying the nonlinear interaction strength. This can be achieved experimentally by exploiting the Feshbach resonances of the BEC, thereby realizing a form of Feshbach engine. Feshbach resonances are a powerful tool used in cold atom experiments, which allow to tune the scattering length of elastic collisions between atoms by using magnetic or optical fields [62]. Such resonances, the thermodynamics of which were recently studied [63], occur when the energy of a bound state of an interatomic potential is equal to the energy of a pair of colliding atoms, resulting in the enhancement of interparticle interactions about the resonace point. To control the time dependence of the interaction, while ensuring suppressed excitations, we use a recently designed STA for this system [25] and investigate its effectiveness by comparing the performance with a suitably rescaled adiabatic modulation. We show that the STA approach leads to higher final target state fidelities and lower irreversible work. We further analyze the engines performance by calculating the efficiency and output power with respect to the cycle duration and find that while arbitrarily fast modulations are ineffective, the STA significantly enhances the overall performance on intermediate timescales. Finally, we highlight the remarkable role that the nonlinear interaction strength plays, showing that due to the effect it has on the energy spectrum, stronger nonlinear interactions allows for increased performance.

The remainder of the paper is organized as follows. In section 2 we present the model and define the thermodynamic quantities used throughout. Section 3 briefly reviews the techniques used to design a STA for dynamically changing the scattering length for soliton matter waves (as devised in [25]) and in section 4 we examine the performance of the STA during a compression. The efficiency and power output of the quantum Otto cycle using the STA is analyzed in section 5 and in section 6 we present our conclusions.

2. Model and figures of merit

We consider the one-dimensional Gross–Pitaevskii equation describing the dynamics of a harmonically trapped BEC

$$\left[-\frac{1}{2}\psi_{xx} + g(t)|\psi(x,\,t)|^2 + \frac{1}{2}x^2\right]\psi(x,\,t) = \mu(t)\psi(x,\,t), \tag{1}$$

where $\psi(x,\,t)$ is the wave-function, $\mu(t)$ is the chemical potential, and $g(t)$ describes the nonlinear interatomic interaction strength, which can be experimentally tuned by applying a Feshbach resonance. Here, we have adopted harmonic oscillator units such that all lengths are scaled by $\sqrt{\hbar/m\omega}$, time t by $1/\omega$, and the interaction strength g by $\sqrt{\hbar^3\omega/m}$, where m is the mass of the condensate and ω is the frequency of the harmonic trapping potential.

In this work we will focus on attractive interactions, $g(t) < 0$, where an exact solution of equation (1) in the absence of the harmonic trap is given by the well-known hyperbolic secant ansatz for a bright soliton matter-wave

$$\psi(x,\,t) = A(t)\,\mathrm{sech}\left(\frac{x}{a(t)}\right). \tag{2}$$

Here, $A(t)$ is the amplitude and $a(t)$ is the width of the soliton, and the system is normalized with respect to the number of particles in the soliton $N = 2aA^2 = \int_{-\infty}^{+\infty} |\psi(x,\,t)|^2 \mathrm{d}x$ with $A = \sqrt{N/(2a)}$. As the width $a(t)$ depends on the interaction strength, varying $g(t)$ leads to compressions and expansions of the soliton. Even though equation (2) is the free-space solution, we will in the following assume that it is still a good approximation in weak trapping potentials.

Varying the interaction strength necessarily implies work being performed on/by the soliton through a change in its energy. The energy of the soliton is given by

$$\epsilon(t) = \int \mathrm{d}x \left[\frac{1}{2}|\nabla\psi(x,\,t)|^2 + \frac{1}{2}x^2|\psi(x,\,t)|^2 - \frac{g(t)}{2}|\psi(x,\,t)|^4\right], \tag{3}$$

where we denote $\epsilon_{i(f)}$ as its initial (final) energy. It therefore follows that the work done during the process is given by the change in the energy

$$W(t) = \epsilon(t) - \epsilon_i. \tag{4}$$

Furthermore, for a quasi-static process the average work done, $\langle W\rangle$, is equal to the adiabatic energy change, $\langle W^{\mathrm{AD}}\rangle$, which in the case of the system being at zero temperature is simply given by the difference between the initial and final energies

$$\langle W\rangle = \langle W^{\mathrm{AD}}\rangle = \epsilon_f - \epsilon_i.$$

Nonadiabatic processes require $\langle W\rangle \geqslant \langle W^{\mathrm{AD}}\rangle$, thus implying that a degree of irreversibility has been introduced. This can be quantified through the irreversible work

$$\langle W_{\mathrm{irr}}\rangle = \langle W\rangle - \langle W^{\mathrm{AD}}\rangle, \tag{5}$$

which in our case is created when applying the control pulses used to manipulate the soliton, as they transiently excite the system. We will use the above quantities to assess the performance of a STA applied to the manipulation of a soliton matter-wave, and its potential use as a small scale engine. For this engine we consider the well-studied Otto cycle as illustrated in figure 1, however since our description of the soliton relies on solving the Gross–Pitaevskii equation which only describes the zero-temperature-state of the system, we make an analogy for the role of temperature in our system. In a physical setting, such a condensed soliton would be surrounded by thermal atoms which would add to the condensate fraction if subsequently cooled. Similarly the condensate fraction of the soliton would decrease with increasing temperature, thus removing particles from the soliton. Situations where quantum bright solitons coexist with free thermal atoms in one-dimensional gases of attractive bosons have recently been a topic of large interest [64–67]. We therefore envisage a particle engine where the compression and expansion strokes are controlled by the interaction strength $g(t)$ and do the work $\langle W_C\rangle$ and $\langle W_E\rangle$ respectively, and the final two strokes of the cycle are at fixed interaction while being coupled to external reservoirs which inserts energy $\langle Q_{N-}\rangle$ or extracts energy $\langle Q_{N+}\rangle$ by removing or adding particles to the soliton.

3. Shortcuts to adiabaticity for soliton matter waves

Compressing or expanding the soliton in a short finite time can create irreversibility in the form out-of-equilibrium excitations, which will hamper the efficiency of the engine cycle. Therefore we aim to employ a STA which will suppress these excitations and ensure the final state has a large overlap with the one that would have been created in a fully adiabatic process. Such a technique was recently developed in [25] and we briefly review it in this section.

For bright solitons the evolution of the width of the cloud, $a(t)$, is related to the nonlinear interaction strength through

$$\ddot{a}(t) + a(t) = \frac{4}{a^3(t)\pi^2} + \frac{2g(t)N}{\pi^2 a^2(t)}, \tag{6}$$

which comes from the variational principle with the hyperbolic secant ansatz, equation (2). To obtain the adiabatic limit, we can solve $\ddot{a} = 0$ from equation (6), to find the dependence of the soliton width on the interaction strength

$$a^4(t) - \frac{2g(t)N}{\pi^2}a(t) = \frac{4}{\pi^2}, \tag{7}$$

which gives an adiabatic reference for the soliton width in terms of the nonlinear interaction in the approximation of a weak trapping potential

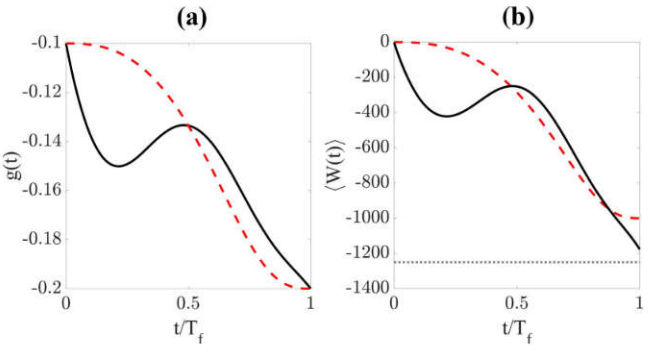

Figure 2. (a) Modulation of the nonlinearity $g(t)$ for a compression stroke. We show the profile as designed by the STA for a finite time stroke $T_f = 0.15$ (solid, black) and for a stroke in the adiabatic limit $T_{\rm AD}$ (dashed, red). We fix $N = 100$. (b) Work done during the compression stroke ($t \leqslant T_f$), when the interaction strength is modulated according to panel (a). We show the STA (solid black) and the TRA stroke (red dashed). The horizontal gray dotted line is the adiabatic energy change $\langle W^{\rm AD}\rangle$.

$$a_c(t) \simeq -\frac{2}{Ng_c(t)}. \tag{8}$$

The above differential equation has a close analogy with the dynamical equation of motion of a fictitious classic particle with position x in a perturbed Kepler problem

$$U(t) \simeq \frac{2g(t)N}{\pi^2 a(t)} + \frac{2}{\pi^2 a^2(t)}. \tag{9}$$

It is worthwhile to note that $a_c(t)$ is indistinguishable from $a(t)$ found from equation (9), corresponding to the minimal energy of Kepler potential, $\partial U(t)/\partial a(t) = 0$.

Using a polynomial ansatz for $a(t)$ given as $a_p(t) = \sum_{i=0}^{5} a_i t^i$, we can fix the boundary conditions for the start, $t = 0$, and end, $t = T_f$, of the stroke as [25]

$$\begin{aligned} a_p(0) &= a_c(0), & a_p(T_f) &= a_c(T_f),\\ \dot{a}_p(0) &= \dot{a}_c(0) = 0, & \dot{a}_p(T_f) &= \dot{a}_c(T_f) = 0,\\ \ddot{a}_p(0) &= \ddot{a}_c(0) = 0, & \ddot{a}_p(T_f) &= \ddot{a}_c(T_f) = 0, \end{aligned} \tag{10}$$

by choosing a smooth adiabatic reference
$g_c(t) = (g_i + g_f)/2 + 9(g_i - g_f)\cos(\pi t/T_f)/16 + (g_f - g_i)\cos(3\pi t/T_f)/16$. Solving this set of equations allows us to determine the coefficients of the polynomial ansatz $a_p(t)$. Setting $a(t) \to a_p(t)$ in equation (6) and rearranging for $g(t)$ we arrive at the desired ramp of the nonlinear interaction strength of a bright soliton matter-wave that realizes a STA for a chosen T_f.

In figure 2(a), we show an example of a ramp of the interaction strength for compression, which corresponds to the pulse that would be applied to achieve one of the adiabatic strokes of the Otto-cycle. Clearly, the functional form of these modulations depends heavily on the total duration of the stroke, T_f and in the adiabatic limit we find $g_{\rm AD}(t) = (\pi^2 a^4(t) - 4)/2Na(t) \simeq -2/Na(t)$ (red, dashed) from equation (7), which is a monotonic function. Conversely, for $T_f = 0.15$ (solid, black) the ramp designed by the STA is more complex, most notably exhibiting a change in slope. This clearly shows that despite achieving essentially the same final state, employing a STA can imply that a drastically different trajectory is followed in order to compensate for the short timescale. In what follows, we will fix T_f and examine the performance of a transformation facilitated by the STA. For comparison we use the same ramp given by the adiabatic limit, but performed in the shorter time T_f, and we refer to this as the time rescaled adiabatic (TRA) stroke. This allows for a fair comparison since as T_f increases, the two modulations coincide.

4. Performance of shortcuts to adiabaticity for soliton compression

We begin by examining the work done during and after a compression from $g_i = -0.1$ to $g_f = -0.2$. Fixing $T_f = 0.15$, we show in figure 2(b) the work for the correctly engineered STA (black) and the TRA (red dashed) stroke. The horizontal dotted line indicates the adiabatic energy change $\langle W^{\rm AD}\rangle$, which is the work done in the perfect adiabatic case. For both approaches, we see that the average work obtained at T_f is different from $\langle W^{\rm AD}\rangle$, which implies that a certain amount of irreversible work was done during each stroke. However, using the STA leads to a significantly smaller degree of irreversibility.

In order to more clearly assess the relative performance of the two strokes, we show the irreversible work, as defined by equation (5), as a function of T_f in figure 3(a). Here the lines show $\langle W_{\rm irr}\rangle$ at the end of the stroke for

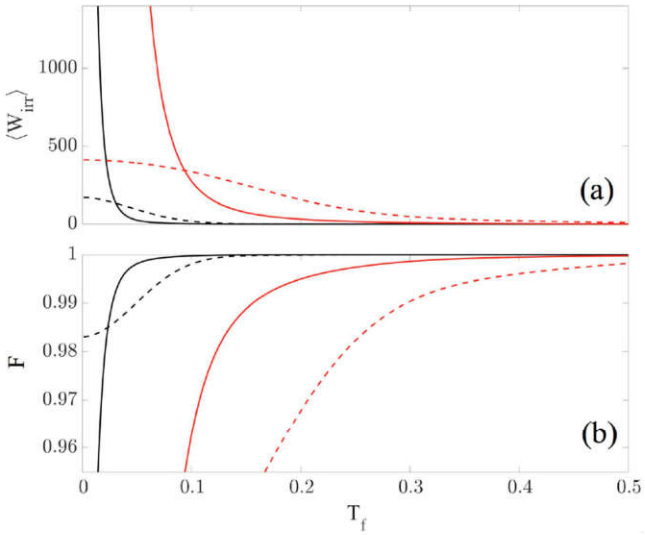

Figure 3. (a) Average irreversible work, $\langle W_{\rm irr}\rangle$ and (b) the final state fidelity, F as a function of T_f. All panels show a compression of the soliton for $g_i = -0.1$ and $g_f = -0.2$ (red lines) and $g_i = -0.2$ and $g_f = -0.2646$ (black lines), with $N = 100$. The solid lines represent the STA while the dashed lines are the TRA strokes.

the STA (solid red) and TRA (dashed red) against T_f for $g_i = -0.1$ and $g_f = -0.2$. Taking larger values of T_f decreases $\langle W_{\rm irr}\rangle$ for both stokes as we approach the adiabatic limit, whereas for small T_f the amount of irreversibility created by both strokes increases. For $T_f \gtrsim 0.1$ the STA creates less irreversible work than the TRA as dynamical excitations are successfully suppressed, however for faster transformation times, $T_f \lesssim 0.1$, we find the converse. This can be understood by considering the modulations that are required by the STA for small T_f, cf figure 2(a). In this case the trajectory for $g(t)$ varies significantly, in stark contrast to the smooth, monotonically decreasing function used for the TRA stroke. This implies the need to input large amounts of energy during the stroke, in turn leading to a significant amount of irreversible work, which diverges as $T_f \to 0$.

To investigate the role of the strength of the nonlinearity in these dynamics we show $\langle W_{\rm irr}\rangle$ for stronger nonlinear interaction strengths $g_i = -0.2$ and $g_f = -0.2646$ as the black curves in figure 3(a). It is important to note that the energy difference between the initial and desired target states here is identical to the previous *weakly* nonlinear case. However, we now see the remarkable role that nonlinearities can play in engineering the STA. The black lines show that, while the qualitative behavior is consistent with the case of weakly nonlinear interactions, the typical values of $\langle W_{\rm irr}\rangle$ that can be achieved are lower. In fact, one can see that using stronger nonlinear interactions allows for significantly faster strokes to be performed while still restricting the creation of excess excitations in the system. The reason for this is the effect that the increased nonlinearity has on the energy spectrum. Larger nonlinearity increases the gap between the energy eigenstates, which in turn allows for a faster driving since the system requires more energy to reach the excited states [33, 35].

A crucial quantity in any control protocol is the final state fidelity, which allows us to quantify how close our final dynamical state at the end of the stroke, $\psi(x,\ T_f)$, is to the target equilibrium state, $\Psi(x)$,

$$F = |\langle \psi(x,\ T_f)\ \Psi(x)\rangle|^2. \tag{11}$$

In figure 3(b) we show that the behavior of F is consistent with the one of $\langle W_{\rm irr}\rangle$, as the STA typically results in larger fidelities at the end of the stroke and therefore gives a more consistent approach to reach the target state than the TRA. Furthermore, using strong nonlinear interactions allows for higher target fidelities at shorter stroke times, however in line with the irreversible work we can see that taking T_f very small leads to the TRA stroke outperforming the STA. Nonetheless, in this case the actual fidelities are quite low in comparison to the desired target state rendering both approaches somewhat ineffective.

From figure 3 we learn three important points: (i) arbitrarily fast manipulation of the soliton matter-wave is not possible using this technique. Such fast manipulation leads to poor final fidelities with the target state, and comes accompanied by sizeable irreversible work. (ii) Stronger non-nonlinear interactions allow for faster strokes. By changing the gaps in the energy spectrum, the larger nonlinear terms lead to better overall performance. (iii) For a realistic implementation, one could fix a minimum average post-stroke fidelity that state must achieve. This will then set a practical lower bound on T_f, which can then be used to determine optimal parameters in order to keep the irreversible work to a minimum.

5. Performance enhanced Otto cycle with a soliton matter wave

While the above analysis only dealt with the compression of the matter-wave, qualitatively similar results hold for an expansion where the nonlinear interaction strength is reduced. However, due to the effect the expansion has on the energy spectrum, this process generally results in slightly lower average fidelities and correspondingly higher irreversible work compared to soliton compression. Regardless, one can use the above approach to assess the performance of a quantum Otto-cycle facilitated using a STA, as depicted in figure 1. To this end, and in line with the analysis of [44, 45] where the case of the exactly solvable harmonic oscillator was treated, we calculate the efficiency of the cycle

$$\eta = -\frac{\langle W_C\rangle + \langle W_E\rangle}{\langle Q_{N_-}\rangle}, \tag{12}$$

where $\langle W_{C(E)}\rangle$ is the work during the compression (expansion) stroke. Here $\langle Q_{N_-}\rangle = \epsilon_E(0, N_E) - \tilde{\epsilon}_C(T_f, N_C)$ is the energy change when particles are lost from the soliton to the free thermal gas, where $\epsilon_E(0, N_E)$ is the initial energy of the soliton before the expansion stroke with N_E particles, while $\tilde{\epsilon}_C(T_f, N_C)$ is the non-adiabatic energy at the end of the compression stroke with N_C particles. Therefore, more particles are condensed in the soliton for the compression than the expansion, $N_C > N_E$, so that when simulating the cycle the effect of temperature is captured by the difference between N_C and N_E. As the normalization of the soliton wavefunction is dependent on $N_{C,E}$, the energy of the soliton will be modified by the change in particle number at end of the work strokes. This is needed to ensure power output from the engine cycle and gives the conditions that $\langle W_E\rangle + \langle W_C\rangle < 0$ and $\langle Q_{N_-}\rangle > 0$. We can immediately see from equation (12) as we reduce the time to perform the strokes, T_f, the efficiency will decrease due to the growing irreversible work created during the STA, see figure 3(a). We also assess the power generated

$$P = -\frac{\langle W_C\rangle + \langle W_E\rangle}{\tau}, \tag{13}$$

where τ is the total time for the whole cycle to be completed. We will assume that the time for the thermalization strokes, where particles are introduced or removed from the system, is much shorter than the time taken for the other strokes to be completed, and therefore $\tau \approx 2T_f$ [41, 44, 45].

Before analyzing these quantities in detail, it is interesting to note that there exists upper bounds on the efficiency and the power by virtue of the QSL, which sets a lower bound on the time required for a quantum state to evolve [26–28, 35, 46] (see [29, 30] for recent reviews). We remark that, although we work with a mean-field dynamics, the QSL is known to extend to classical settings [68–70]. In the present context we can define the QSL as

$$T_f > T^{\rm QSL} = \frac{\hbar B}{\langle \mathcal{E}_{\rm STA}\rangle}, \tag{14}$$

where B is the Bures angle between the initial and final states [28] and $\langle \mathcal{E}_{\rm STA}\rangle = \frac{1}{T_f}\int_0^{T_f}[\epsilon^I_{\rm STA}(t) - \epsilon^I_{\rm TRA}(t)]\,{\rm d}t$ is the energy of the shortcut, where $\epsilon^I_{\rm STA}(t)$ ($\epsilon^I_{\rm TRA}(t)$) is the energy of the instantaneous eigenstate for the value of $g(t)$ for the STA (TRA). As shown in [44, 45] the upper bounds are then given by

$$\eta_{\rm QSL} = -\frac{\langle W_C^{\rm AD}\rangle + \langle W_E^{\rm AD}\rangle}{\langle Q_{N_-}\rangle + \hbar\,(B_C + B_E)/\tau}, \tag{15}$$

$$P_{\rm QSL} = -\frac{\langle W_C^{\rm AD}\rangle + \langle W_E^{\rm AD}\rangle}{T_C^{\rm QSL} + T_E^{\rm QSL}}, \tag{16}$$

where B_C and B_E are the the Bures angles for the compression and expansion strokes, and $\langle W^{\rm AD}_{C,E}\rangle$ is the adiabatic work difference for compression or expansion of the soliton. The thin dotted curves in figure 4 correspond to these upper bounds.

We examine the efficiency and power of the Otto cycle in figure 4 for weak (red) and strong (black) nonlinear interaction strengths for the STA (solid) and the TRA (dashed) strokes, while the compression and expansion strokes are implemented with solitons composed of $N_C = 100$ and $N_E = 90$ particles respectively. As done previously, to ensure a fair comparison, the magnitude of the change in the nonlinear interaction is modified such that in the adiabatic limit the work performed during each stroke of the two realizations is the same. Furthermore, the power in the adiabatic limit for the two interaction regimes will also be identical and we rescale η with respect to the adiabatic efficiency, $\eta_{\rm AD}$. We see that the efficiency is always poor for small T_f, regardless of the interaction regime or the type of ramp applied. Larger T_f allows one to realize a significantly more efficient cycle, one that operates at close to the adiabatic efficiency and, on these timescales, we find the use of the STA is always advantageous. Furthermore, we again see that stronger nonlinearities lead to a better overall performance, while the output power is more sharply peaked and experiences a sharp cutoff. This is a consequence of the increased slope of $\langle W_{\rm irr}\rangle$ at short T_f, as the designed STA must approach $g \to 0$ to

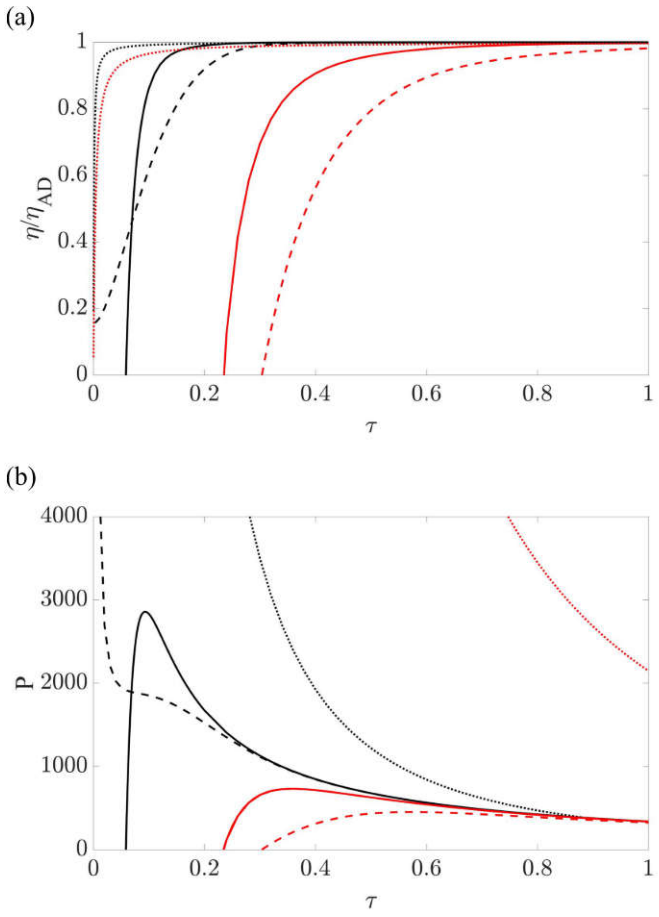

Figure 4. (a) Efficiency of the cycle normalized with respect to the adiabatic efficiency η_{AD} and (b) power, for the weakly nonlinear case with $g_i = -0.1$ and $g_f = -0.2$ (red lines, $\eta_{AD} \approx 0.76$) and strongly nonlinear case $g_i = -0.2$ and $g_f = -0.2646$ (black lines, $\eta_{AD} \approx 0.43$). The solid lines represent the STA while the dashed lines are the corresponding TRA stroke. The thin dotted lines are the respective upper bounds dictated by the QSL. Along the compression stroke we take $N_C = 100$ while along the expansion stroke we fix $N_E = 90$.

compensate for the excess energy put into the system. For $|gN| \approx 1$ the sech ansatz for the soliton breaks down and the STA becomes ineffective. Finally, comparing with the bounds defined by the QSL, we see that for intermediate timescales strong nonlinearities allow for an efficiency and power close to maximal. As we increase T_f, and all protocols approach the adiabatic limit, we find the curves all converge on top of one-another.

An important caveat must be stressed regarding the above results. Our definitions of efficiency and power do not account for any cost (energetic or otherwise) in achieving the desired dynamics. Such a question has received intense interest recently [33–36, 44–47]. A reasonable (although not unique) definition for the cost of achieving one of the expansion/compression strokes is to determine the energy required for the pulse, i.e. $\langle \mathcal{E}_{\rm STA} \rangle$. As this represents an additional energy input, the efficiency then becomes

$$\eta_{\rm cost} = -\frac{\langle W_C \rangle + \langle W_E \rangle}{\langle Q_{N_-} \rangle + \langle \mathcal{E}_{\rm STA} \rangle_C + \langle \mathcal{E}_{\rm STA} \rangle_E}. \tag{17}$$

Including this additional energy term should also have an effect on the output power. Indeed, if we view the use of the STA as a means to boost performance, the added power inputted through the use of the pulse should be subtracted from the total output power, thus

$$P_{\rm cost} = -\frac{\langle W_C \rangle + \langle W_E \rangle - \langle \mathcal{E}_{\rm STA} \rangle_C - \langle \mathcal{E}_{\rm STA} \rangle_E}{\tau}. \tag{18}$$

In figure 5 we compare these quantities to equations (12) and (13). Clearly, the qualitative behavior is consistent, with the overall effect to slightly decrease the performance. However, we see that the advantages pointed out previously still persist, allowing us to conclude that even by including the additional energy required to achieve the dynamics, the STA can still significantly boost the performance of the cycle. As a final remark, while there are several (related) definitions for the cost required to achieve a STA currently in the literature [33–36, 44–47], regardless of which approach is chosen the general features outlined here will persist.

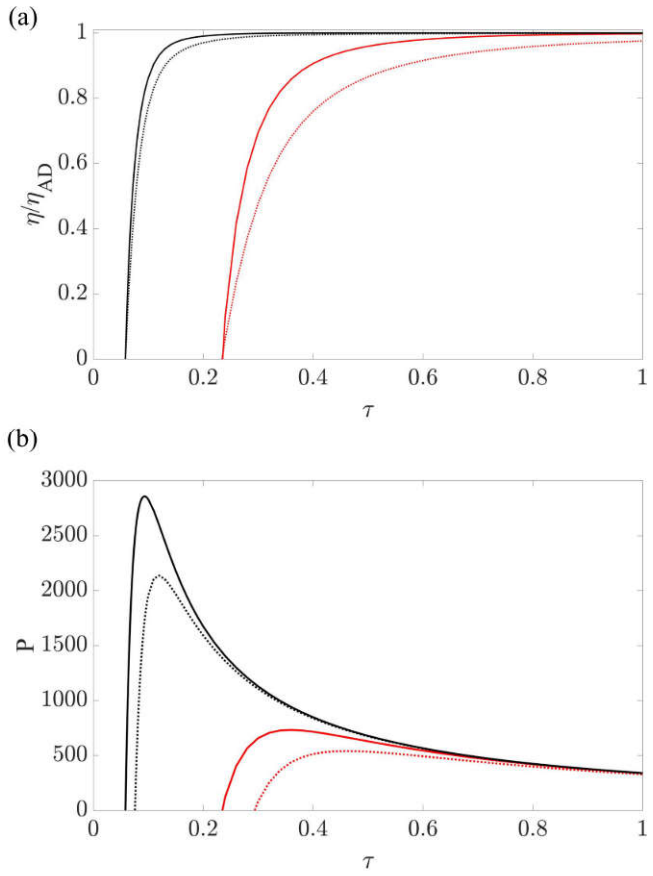

Figure 5. (a) Efficiency of the cycle normalized with respect to the adiabatic efficiency η_{AD} and (b) power, for the weakly nonlinear case with $g_i = -0.1$ and $g_f = -0.2$ (red lines, $\eta_{AD} \approx 0.76$) and strongly nonlinear case $g_i = -0.2$ and $g_f = -0.2646$ (black lines, $\eta_{AD} \approx 0.43$). The solid lines represent efficiency and power calculated with equations (12) and (13) respectively. The thin dotted lines are efficiency and power calculated with equations (17) and (18) respectively, which includes the added energy required to implement the STA.

6. Conclusions

We have analyzed the performance of a recently proposed STA which modulates the nonlinear interaction of a soliton matter wave. We quantified the effectiveness of the STA during compression of the soliton by calculating the irreversible work and the fidelity of the final state. We showed that the STA is a viable technique to efficiently suppresses excitations on non-adiabatic timescales, while its use on arbitrarily short timescales results in the generation of a significant degree of irreversibility when implementing the STA. Examining the performance of an Otto cycle using the soliton matter-wave as a working substance, we have shown that the STA can be a useful tool for these intermediate timescales, and that larger nonlinear interaction strengths lead to a better overall performance. Our results thus significantly add to the study of quantum thermal cycles by taking advantage of the versatility of BECs to create a Feshbach engine, which can be efficiently controlled by tuning the nonlinearity according to the STA. This system is also experimentally viable, where the energy of the soliton can be extracted from *in situ* observations of the density, or through time-of-flight measurements of the momentum distribution.

Acknowledgments

We thank Sebastian Deffner for insightful discussions. This work was supported by the Okinawa Institute of Science and Technology Graduate University. We acknowledge support from the NSFC (11474193), the Shuguang program (14SG35), the Program for Professor of Special Appointment (Eastern Scholar), and the COST Action MP1209 'Thermodynamics in the Quantum Regime'.

ORCID iDs

Thomás Fogarty https://orcid.org/0000-0003-4940-5861
Steve Campbell https://orcid.org/0000-0002-3427-9113
Xi Chen https://orcid.org/0000-0003-4221-4288
Thomas Busch https://orcid.org/0000-0003-0535-2833

References

[1] Campisi M, Hänggi P and Talkner P 2011 Colloquium: Quantum fluctuation relations: foundations and applications *Rev. Mod. Phys.* **83** 771–91
[2] Goold J, Huber M, Riera A, del Rio L and Skrzypczyk P 2016 The role of quantum information in thermodynamics—a topical review *J. Phys. A: Math. Theor.* **49** 143001
[3] Fusco L, Pigeon S, Apollaro T J G, Xuereb A, Mazzola L, Campisi M, Ferraro A, Paternostro M and De Chiara G 2014 Assessing the nonequilibrium thermodynamics in a quenched quantum many-body system via single projective measurements *Phys. Rev.* X **4** 031029
[4] Martinez I A, Petrosyan A, Guéry-Odelin D, Trizac E and Ciliberto S 2016 Engineered swift equilibration of a Brownian particle *Nat. Phys.* **12** 843–6
[5] Hansel W, Hommelhoff P, Hansch T W and Reichel J 2001 Bose–Einstein condensation on a microelectronic chip *Nature* **413** 498–501
[6] Bulatov A, Vugmeister B E and Rabitz H 1999 Nonadiabatic control of Bose–Einstein condensation in optical traps *Phys. Rev.* A **60** 4875–81
[7] Couvert A, Kawalec T, Reinaudi G and Guéry-Odelin D 2008 Optimal transport of ultracold atoms in the non-adiabatic regime *Europhys. Lett.* **83** 13001
[8] Léonard J, Lee M, Morales A, Karg T M, Esslinger T and Donner T 2014 Optical transport and manipulation of an ultracold atomic cloud using focus-tunable lenses *New J. Phys.* **16** 093028
[9] Bücker R, Berrada T, van Frank S, Schaff J-F, Schumm T, Schmiedmayer J, Jäger G, Grond J and Hohenester U 2013 Vibrational state inversion of a Bose–Einstein condensate: optimal control and state tomography *J. Phys. B: At. Mol. Opt. Phys.* **46** 104012
[10] Fialko O and Hallwood D W 2012 Isolated quantum heat engine *Phys. Rev. Lett.* **108** 085303
[11] Abah O, Roßnagel J, Jacob G, Deffner S, Schmidt-Kaler F, Singer K and Lutz E 2012 Single-ion heat engine at maximum power *Phys. Rev. Lett.* **109** 203006
[12] Rossnagel J, Dawkins S T, Tolazzi K N, Abah O, Lutz E, Schmidt-Kaler F and Singer K 2016 A single-atom heat engine *Science* **352** 325–9
[13] Muga J G, Chen X, Ruschhaupt A and Guéry-Odelin D 2009 Frictionless dynamics of Bose–Einstein condensates under fast trap variations *J. Phys. B: At. Mol. Opt. Phys.* **42** 241001
[14] Chen X, Ruschhaupt A, Schmidt S, del Campo A, Guéry-Odelin D and Muga J G 2010 Fast optimal frictionless atom cooling in harmonic traps: shortcut to adiabaticity *Phys. Rev. Lett.* **104** 063002
[15] Schaff J-F, Song X-L, Vignolo P and Labeyrie G 2010 Fast optimal transition between two equilibrium states *Phys. Rev.* A **82** 033430
[16] Schaff J-F, Song X-L, Capuzzi P, Vignolo P and Labeyrie G 2011 Shortcut to adiabaticity for an interacting Bose–Einstein condensate *Europhys. Lett.* **93** 23001
[17] Schaff J-F, Capuzzi P, Labeyrie G and Vignolo P 2011 Shortcuts to adiabaticity for trapped ultracold gases *New J. Phys.* **13** 113017
[18] Torrontegui E, Ibáñez S, Martínez-Garaot S, Modugno M, del Campo A, Guéry-Odelin D, Ruschhaupt A, Chen X and Muga J G 2013 Shortcuts to adiabaticity *Adv. At. Mol. Opt. Phys.* **62** 117
[19] Deffner S, Jarzynski C and del Campo A 2014 Classical and quantum shortcuts to adiabaticity for scale-invariant driving *Phys. Rev.* X **4** 021013
[20] del Campo A 2011 Fast frictionless dynamics as a toolbox for low-dimensional Bose–Einstein condensates *Europhys. Lett.* **96** 60005
[21] Rohringer W, Fischer D, Steiner F, Mazets I E, Schmiedmayer J and Trupke M 2015 Non-equilibrium scale invariance and shortcuts to adiabaticity in a one-dimensional bose gas *Sci. Rep.* **5** 9820
[22] Campbell S, De Chiara G, Paternostro M, Palma G M and Fazio R 2015 Shortcut to adiabaticity in the Lipkin–Meshkov–Glick model *Phys. Rev. Lett.* **114** 177206
[23] Guéry-Odelin D, Muga J G, Ruiz-Montero M J and Trizac E 2014 Nonequilibrium solutions of the Boltzmann equation under the action of an external force *Phys. Rev. Lett.* **112** 180602
[24] Papoular D J and Stringari S 2015 Shortcut to adiabaticity for an anisotropic gas containing quantum defects *Phys. Rev. Lett.* **115** 025302
[25] Li J, Sun K and Chen X 2016 Shortcut to adiabatic control of soliton matter waves by tunable interaction *Sci. Rep.* **6** 38258
[26] Mandelstam L and Tamm I 1945 The uncertainty relation between energy and time in nonrelativistic quantum mechanics *J. Phys.* **9** 249
[27] Margolus N and Levitin L B 1998 The maximum speed of dynamical evolution *Physica* D **120** 188
[28] Deffner S and Lutz E 2013 Quantum speed limit for non-Markovian dynamics *Phys. Rev. Lett.* **111** 010402
[29] Frey M R 2016 Quantum speed limits—primer, perspectives, and potential future directions *Quantum Inf. Process.* **15** 3919
[30] Deffner S and Campbell S 2017 Quantum speed limits: from Heisenberg's uncertainty principle to optimal quantum control *J. Phys. A: Math. Theor.* **50** 453001
[31] Chen X and Muga J G 2010 Transient energy excitation in shortcuts to adiabaticity for the time-dependent harmonic oscillator *Phys. Rev.* A **82** 053403
[32] Cui Y-Y, Chen X and Muga J G 2016 Transient particle energies in shortcuts to adiabatic expansions of harmonic traps *J. Phys. Chem.* A **120** 2962–9
[33] Zheng Y, Campbell S, De Chiara G and Poletti D 2016 Cost of counterdiabatic driving and work output *Phys. Rev.* A **94** 042132
[34] Santos A C and Sarandy M S 2015 Superadiabatic controlled evolutions and universal quantum computation *Sci. Rep.* **5** 15775
[35] Campbell S and Deffner S 2017 Trade-off between speed and cost in shortcuts to adiabaticity *Phys. Rev. Lett.* **118** 100601
[36] Torrontegui E, Lizuain I, González-Resines S, Tobalina A, Ruschhaupt A, Kosloff R and Muga J G 2017 Energy consumption for shortcuts to adiabaticity *Phys. Rev.* A **96** 022133
[37] Coulamy I B, Santos A C, Hen I and Sarandy M S 2016 Energetic cost of superadiabatic quantum computation *Front. ICT* **3** 19
[38] Santos A C and Sarandy M S 2017 Generalized shortcuts to adiabaticity and enhanced robustness against decoherence arXiv:1702.02239
[39] Rezek Y, Salamon P, Hoffmann K H and Kosloff R 2009 The quantum refrigerator: the quest for absolute zero *Europhys. Lett.* **85** 30008

[40] Hoffmann K H, Salamon P, Rezek Y and Kosloff R 2011 Time-optimal controls for frictionless cooling in harmonic traps *Europhys. Lett.* **96** 60015
[41] del Campo A, Goold J and Paternostro M 2014 More bang for your buck: towards super-adiabatic quantum engines *Sci. Rep.* **4** 6208
[42] Deng J, Wang Q-H, Liu Z, Hänggi P and Gong J 2013 Boosting work characteristics and overall heat-engine performance via shortcuts to adiabaticity: quantum and classical systems *Phys. Rev.* E **88** 062122
[43] Beau M, Jaramillo J and del Campo A 2016 Scaling-up quantum heat engines efficiently via shortcuts to adiabaticity *Entropy* **18** 168
[44] Abah O and Lutz E 2017 Energy efficient quantum machines *Europhys. Lett.* **118** 40005
[45] Abah O and Lutz E 2017 Performance of shortcut-to-adiabaticity quantum engines arXiv:1707.09963
[46] Funo K, Zhang J-N, Chatou C, Kim K, Ueda M and del Campo A 2017 Universal work fluctuations during shortcuts to adiabaticity by counterdiabatic driving *Phys. Rev. Lett.* **118** 100602
[47] Kosloff R and Rezek Y 2017 The quantum harmonic Otto cycle *Entropy* **19** 136
[48] Kosloff R 1984 A quantum mechanical open system as a model of a heat engine *J. Chem. Phys.* **80** 1625–31
[49] Quan H T, Liu Y-x, Sun C P and Nori F 2007 Quantum thermodynamic cycles and quantum heat engines *Phys. Rev.* E **76** 031105
[50] Abah O and Lutz E 2014 Efficiency of heat engines coupled to nonequilibrium reservoirs *Europhys. Lett.* **106** 20001
[51] Abah O and Lutz E 2016 Optimal performance of a quantum Otto refrigerator *Europhys. Lett.* **113** 60002
[52] Zhang K, Bariani F and Meystre P 2014 Quantum optomechanical heat engine *Phys. Rev. Lett.* **112** 150602
[53] Zheng Y and Poletti D 2015 Quantum statistics and the performance of engine cycles *Phys. Rev.* E **92** 012110
[54] Altintas F and Mustecaplioglu O E 2015 General formalism of local thermodynamics with an example: quantum Otto engine with a spin-1/2 coupled to an arbitrary spin *Phys. Rev.* E **92** 022142
[55] Reid B, Pigeon S, Antezza M and Chiara G De 2017 A self-contained quantum harmonic engine arXiv:1708.07435
[56] Aycock L M, Hurst H M, Efimkin D K, Genkina D, Lu H-I, Galitski V M and Spielman I B 2017 Brownian motion of solitons in a Bose–Einstein condensate *Proc. Natl Acad. Soc.* **114** 2503–8
[57] Strecker K E, Partridge G B, Truscott A G and Hulet R G 2002 Formation and propagation of matter-wave soliton trains *Nature* **417** 150–3
[58] Khaykovich L, Schreck F, Ferrari G, Bourdel T, Cubizolles J, Carr L D, Castin Y and Salomon C 2002 Formation of a matter-wave bright soliton *Science* **296** 1290–3
[59] Marchant A L, Billam T P, Wiles T P, Yu M M H, Gardiner S A and Cornish S L 2013 Controlled formation and reflection of a bright solitary matter-wave *Nat. Commun.* **4** 1865
[60] Marchant A L, Billam T P, Yu M M H, Rakonjac A, Helm J L, Polo J, Weiss C, Gardiner S A and Cornish S L 2016 Quantum reflection of bright solitary matter waves from a narrow attractive potential *Phys. Rev.* A **93** 021604
[61] Nguyen J H V, Luo D and Hulet R G 2017 Formation of matter-wave soliton trains by modulational instability *Science* **356** 422–6
[62] Chin C, Grimm R, Julienne P and Tiesinga E 2010 Feshbach resonances in ultracold gases *Rev. Mod. Phys.* **82** 1225–86
[63] García-March M A, Fogarty T, Campbell S, Busch T and Paternostro M 2016 Non-equilibrium thermodynamics of harmonically trapped bosons *New J. Phys.* **18** 103035
[64] Herzog C, Olshanii M and Castin Y 2014 A liquid–gas transition for bosons with attractive interaction in one dimension *C. R. Phys.* **15** 285–96
[65] Weiss C, Gardiner S A and Gertjerenken B 2016 Temperatures are not useful to characterise bright-soliton experiments for ultra-cold atoms arXiv:1610.09074
[66] Weiss C 2016 Finite-temperature phase transition in a homogeneous one-dimensional gas of attractive bosons arXiv:1610.09070
[67] Weiss C and Carr L D 2016 Higher-order quantum bright solitons in Bose–Einstein condensates show truly quantum emergent behavior arXiv:1612.05545
[68] Deffner S 2017 Geometric quantum speed limits: a case for Wigner phase space *New J. Phys.* **19** 103018
[69] Bravetti A and Tapias D 2017 *Phys. Rev.* E **96** 052107
[70] Okuyama M and Ohzeki M 2017 Quantum speed limit is not quantum arXiv:1710.03498